Development of Indolequinone Mechanism-Based Inhibitors of NAD(P)H:Quinone Oxidoreductase 1 (NQO1): NQO1 Inhibition and Growth Inhibitory Activity in Human Pancreatic MIA PaCa-2 Cancer Cells†

Philip Reigan,‡ Marie A. Colucci,§ David Siegel,‡ Aurélie Chilloux,§ Christopher J. Moody,§ and David Ross*,‡

Department of Pharmaceutical Sciences and Cancer Center, School of Pharmacy, University of Colorado at Denver and Health Sciences Center, Denver, Colorado 80262, and School of Chemistry, University of Nottingham, University Park, Nottingham, NG7 2RD U.K.

Received January 2, 2007; Revised Manuscript Received March 1, 2007

ABSTRACT: NAD(P)H:quinone oxidoreductase 1 (NQO1) is currently an emerging target in pancreatic cancer. In this report, we describe a series of indolequinones, based on 5-methoxy-1,2-dimethyl-3-[(4-nitrophenoxy)methyl]indole-4,7-dione (ES936), and evaluate NQO1 inhibition and growth inhibitory activity in the human pancreatic MIA PaCa-2 tumor cell line. The indolequinones with 4-nitrophenoxy, 4-pyridinyloxy, and acetoxy substituents at the (indol-3-yl)methyl position were NADH-dependent inhibitors of recombinant human NQO1, indicative of mechanism-based inhibition. However, those with hydroxy and phenoxy substituents were poor inhibitors of NQO1 enzyme activity, due to attenuated elimination of the leaving group. The ability of this series of indolequinones to inhibit recombinant human NQO1 correlated with NQO1 inhibition in MIA PaCa-2 cells. The examination of indolequinone interactions in complex with NQO1 from computational-based molecular docking simulations supported the observed biochemical data with respect to NQO1 inhibition. The design of both NQO1-inhibitory and noninhibitory indolequinone analogues allowed us to test the hypothesis that NQO1 inhibition was required for growth inhibitory activity in MIA PaCa-2 cells. ES936 and its 6-methoxy analogue were potent inhibitors of NQO1 activity and cell proliferation; however, the 4-pyridinyloxy and acetoxy compounds were also potent inhibitors of NQO1 activity but relatively poor inhibitors of cell proliferation. In addition, the phenoxy compounds, which were not inhibitors of NQO1 enzymatic activity, demonstrated potent growth inhibition. These data demonstrate that NQO1 inhibitory activity can be dissociated from growth inhibitory activity and suggest additional or alternative targets to NQO1 that are responsible for the growth inhibitory activity of this series of indolequinones in human pancreatic cancer.

NAD(P)H:quinone oxidoreductase 1 (NQO1,[1] EC 1.6.99.2, DT-diaphorase) is a cytosolic homodimeric flavoprotein containing one FAD site per monomer that utilizes NADH or NADPH to catalyze the direct two-electron reduction of a broad range of quinone substrates to the corresponding hydroquinone (*1*, *2*). Two-electron reduction evades one-electron reduction and the formation of the highly reactive semiquinone radical intermediate preventing redox cycling and the generation of reactive oxygen species (*2*−*4*). In contrast to the chemoprotective role of NQO1, the enzyme also catalyzes the bioactivation of antitumor quinones such as mitomycin C and EO9 (*5*, *6*), which exert their toxicity through direct DNA damage. Cancer cells expressing high levels of NQO1 accumulate greater levels of these activated antitumor quinones, increasing their antitumor efficacy. Elevated levels of NQO1 expression have been documented in a variety of human tumors, including breast, colon, lung, ovary, thyroid, adrenal gland, and liver, when compared with normal tissues of the same origin (*7*−*9*). NQO1 is also overexpressed in pancreatic cancer as demonstrated by immunohistochemical, immunocytochemical, and quantitative RT-PCR techniques (*10*, *11*). Microarray gene expression profiling in pancreatic adenocarcinoma, pancreatitis, pancreatic cancer cell lines, and normal pancreas exhibited a 12-fold increase of NQO1 expression in pancreatic tumors compared to normal pancreas (*10*, *11*). Pancreatic cancer represents the fifth leading cause of cancer death in the United States (*12*, *13*), and a steady increase in the occurrence of pancreatic cancer has been recorded in females in a number of Western countries (*14*). There are currently very

† This work was supported by National Institutes of Health Grant RO1 CA114441, the Association for International Cancer Research (AICR), and the FORCE cancer charity.

* To whom correspondence should be addressed. E-mail: david.ross@uchsc.edu. Tel: 303-315-6077. Fax: 303-315-6281.

‡ University of Colorado at Denver and Health Sciences Center.

§ University of Nottingham.

[1] Abbreviations: NQO1, NAD(P)H quinone:oxidoreductase 1; FAD, flavin adenine dinucleotide; **1** (ES936), 5-methoxy-1,2-dimethyl-3-[(4-nitrophenoxy)methyl]indole-4,7-dione; **2**, 6-methoxy-1,2-dimethyl-3-[(4-nitrophenoxy)methyl]indole-4,7-dione; **3**, 5-methoxy-1,2-dimethyl-3-[(phenoxy)methyl]indole-4,7-dione; **4**, 6-methoxy-1,2-dimethyl-3-[(phenoxy)methyl]indole-4,7-dione; **5**, 5-methoxy-1,2-dimethyl-3-[(4-pyridinyloxy)methyl]indole-4,7-dione; **6**, 6-methoxy-1,2-dimethyl-3-[(4-pyridinyloxy)methyl]indole-4,7-dione; **7**, 6-methoxy-1,2-dimethyl-3-[(acetoxy)methyl]indole-4,7-dione; **8**, 5-methoxy-1,2-dimethyl-3-(hydroxymethyl)indole-4,7-dione; **9**, 6-methoxy-1,2-dimethyl-3-(hydroxymethyl)indole-4,7-dione; rh, recombinant human; PDB, Protein Data Bank; RCSB, Research Collaboratory for Structural Bioinformatics; CVFF, consistent valence force field.

10.1021/bi700008y CCC: $37.00
Published on Web 04/25/2007

Scheme 1: NQO1-Mediated Reduction of Indolequinones[a]

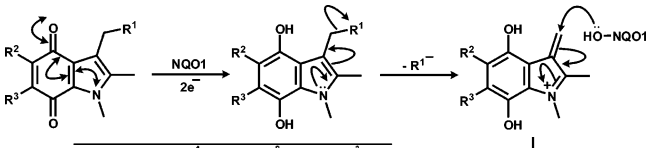

Compound	R^1	R^2	R^3
1 (ES936)	$OC_6H_4NO_2$	OCH_3	H
2	$OC_6H_4NO_2$	H	OCH_3
3	OC_6H_5	OCH_3	H
4	OC_6H_5	H	OCH_3
5	OC_5H_4N	OCH_3	H
6	OC_5H_4N	H	OCH_3
7	$OCOCH_3$	H	OCH_3
8	OH	OCH_3	H
9	OH	H	OCH_3

[a] Reduction of the indolequinone leads to formation of the hydroquinone and the elimination of the leaving group and the generation of an iminium ion alkylating species, where X = H or protein.

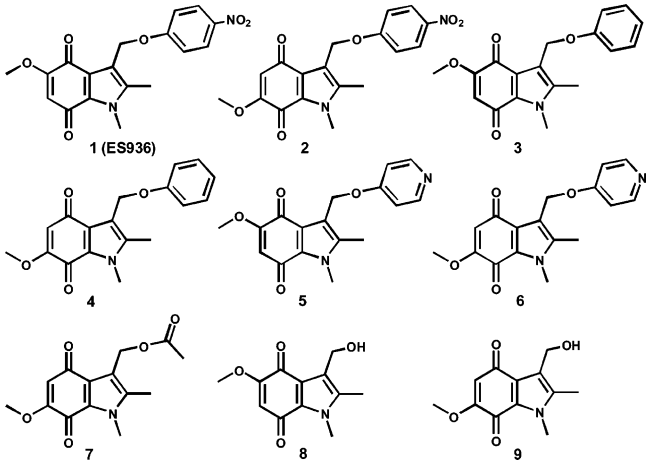

FIGURE 1: Structures of the indolequinone compounds.

few early biomarkers to detect pancreatic cancer, although human epidemiological studies have associated pancreatic cancer with dietary factors, cigarette smoking, and aging (*15*, *16*). Once diagnosed, pancreatic cancer has a prognosis that is virtually terminal within 5 years (*17*), and current treatments of radiation therapy, chemotherapy, and surgery have been ineffective at improving the survival rate (*18*−*21*). The aggressive malignancy, poor prognosis, and increasing incidence of this cancer type necessitate the development of effective targeted therapeutic treatments.

Recently, the inhibition of NQO1, using the anticoagulant dicumarol, has been proposed to result in increased cellular superoxide and the suppression of the malignant phenotype in human pancreatic cancer cells (*22*). This approach would represent a novel strategy for the treatment of mammalian tumors expressing NQO1 where inhibition of NQO1 leads to cell death through accumulation of intracellular superoxide, and in support of this proposed mechanism we have recently demonstrated that NQO1 can directly scavenge superoxide (*23*). However, dicumarol is a nonspecific, competitive inhibitor of NQO1, known to have many ancillary effects in addition to inhibition of NQO1 (*6*, *24*−*27*). Therefore, there is a need to develop specific potent inhibitors of NQO1 as a potential treatment for pancreatic cancer.

In previous studies, 5-methoxy-1,2-dimethyl-3-[(4-nitrophenoxy)methyl]indole-4,7-dione (ES936, **1**) has demonstrated mechanism-based inhibition of NQO1, both in vitro and in vivo (*28*−*31*). The NQO1-mediated bioreduction of this type of indolequinone, has been reported to induce the efficient elimination of various leaving groups, such as a phenol or carboxylic acid, from the (indol-3-yl)methyl position (*32*), generating the reactive iminium ion species (Scheme 1). In the case of ES936, reductive activation by NQO1 facilitates the elimination of the 4-nitrophenoxy group with the subsequent generation of a reactive iminium ion intermediate, which then alkylates either Tyr126 or Tyr128 within the FAD site (*29*) of NQO1, thereby inhibiting quinone reductase activity. More recently, we have reported the effect of this mechanism-based inhibition of NQO1 in the human pancreatic BxPC-3 and MIA PaCa-2 tumor cell lines and demonstrated that the associated cytotoxicity was independent of superoxide generation (*33*). The dissociation of superoxide generation from cytotoxicity allows for potential additional effects other than NQO1 inhibition contributing to the overall mechanism of action of these indolequinones in pancreatic cancer. We have therefore designed a structure−activity study to resolve NQO1 inhibition as a potential anticancer therapy.

In the present study, we have examined a series of indolequinones, **1**−**9** (Figure 1), based on ES936 (**1**) and its 6-methoxy-1,2-dimethyl-3-[(4-nitrophenoxy)methyl]indole-4,7-dione (**2**) analogue and include 5-methoxy-1,2-dimethyl-3-[(phenoxy)methyl]indole-4,7-dione (**3**), 6-methoxy-1,2-dimethyl-3-[(phenoxy)methyl]indole-4,7-dione (**4**), 5-methoxy-1,2-dimethyl-3-[(4-pyridinyloxy)methyl]indole-4,7-dione (**5**), 6-methoxy-1,2-dimethyl-3-[(4-pyridinyloxy)methyl]indole-4,7-dione (**6**), 6-methoxy-1,2-dimethyl-3-[(acetoxy)methyl]-indole-4,7-dione (**7**), 5-methoxy-1,2-dimethyl-3-(hydroxymethyl)indole-4,7-dione (**8**), and 6-methoxy-1,2-dimethyl-3-(hydroxymethyl)indole-4,7-dione (**9**). Some of the indolequinones, in this series, were designed to act as mechanism-based inhibitors of NQO1, which was supported by biochemical studies of NQO1 inhibition using both recombinant human enzyme and MIA PaCa-2 human pancreatic cancer cells and theoretical molecular docking simulations in the human NQO1 crystal structure. We tested the hypothesis that NQO1 inhibition was required for growth inhibition induced by these indolequinones in the MIA PaCa-2 pancreatic cancer cell line. Our data demonstrate that NQO1 inhibition can be dissociated from growth inhibition, suggesting the need for additional or alternative targets to NQO1 to explain the potent activity of this series of indolequinones in pancreatic tumor cells.

MATERIALS AND METHODS

Materials. NADH, FAD, 2,6-dichlorophenolindophenol (DCPIP), 3-(4,5-dimethylthiazol-2-yl)-2,5-diphenyltetrazolium bromide (MTT), bovine serum albumin, and streptonigrin were obtained from Sigma Chemical Co. (St. Louis, MO). The indolequinones 5-methoxy-1,2-dimethyl-3-[(4-nitrophenoxy)methyl]indole-4,7-dione (ES936, **1**), 6-methoxy-1,2-dimethyl-3-[(4-nitrophenoxy)methyl]indole-4,7-dione (**2**), 5-methoxy-1,2-dimethyl-3-[(phenoxy)methyl]indole-4,7-dione (**3**), 6-methoxy-1,2-dimethyl-3-[(phenoxy)methyl]indole-4,7-dione (**4**), 5-methoxy-1,2-dimethyl-3-[(4-pyridinyloxy) methyl]indole-4,7-dione (**5**), 6-methoxy-1,2-dimethyl-3-[(4-pyridinyloxy)methyl]indole-4,7-dione (**6**), 6-methoxy-1,2-dimethyl-3-[(acetoxy)methyl]indole-4,7-dione (**7**), 5-meth-

oxy-1,2-dimethyl-3-(hydroxymethyl)indole-4,7-dione (**8**), and 6-methoxy-1,2-dimethyl-3-(hydroxymethyl)indole-4,7-dione (**9**) were synthesized in the laboratory of Professor C. J. Moody. rhNQO1 was purified from *Escherichia coli* using Cibacron blue affinity chromatography as previously described (*34*) and had a specific activity of 800 μmol of DCPIP min^{-1} (mg of protein)$^{-1}$.

Cell Lines. Human pancreatic MIA PaCa-2 carcinoma cells were obtained from ATCC (Manassas, VA) and grown in Dulbecco's modified Eagle's medium adjusted to contain 4 mM L-glutamine, 1.5 g/L sodium bicarbonate, 4.5 g/L glucose (78.8%), 14% (v/v) fetal bovine serum, 2.5% (v/v) horse serum, 100 units/mL penicillin, and 100 μg/mL streptomycin. Cells were maintained in a humidified incubator containing 5% carbon dioxide at 37 °C.

NQO1 Inactivation. The mechanism-based inactivation of rhNQO1 by this indolequinone series was assayed using the following methods. In these reactions (0.5 mL final volume) rhNQO1 (2 μg/mL) was incubated with 0.1−5.0 μM indolequinone in the absence and presence of 0.2 mM NADH in 50 mM potassium phosphate buffer, pH 7.4, containing 125 mM NaCl and 1 mg/mL bovine serum albumin at 32 °C. After 5 min a 50 μL aliquot was removed and diluted 100-fold in stop buffer [50 mM potassium phosphate buffer, pH 7.4, containing 250 mM sucrose, 5 μM FAD, and 0.1% (v/v) Tween-20], 960 μL was transferred to a cuvette with 0.2 mM NADH and 40 μM DCPIP (final volume 1 mL), and the linear decrease in absorbance was monitored at 600 nm for 1 min at 32 °C. Partition ratios for the inactivation of rhNQO1 by the indolequinones that demonstrated mechanism-based inhibition were determined essentially as described above except that the compounds and rhNQO1 were incubated in the presence of 0.2 mM NADH for 15 min, with defined molar ratios of indolequinone to rhNQO1 (range 0.2:1 to 1250:1). Inactivation of NQO1 in MIA PaCa-2 cells in culture by these indolequinones was determined using the following procedure. Cells were grown to 80−90% confluency in 60 mm plates with 5 mL of complete medium. Growth medium was replaced with the indolequinone containing complete medium for a 1 or 4 h time period, after which the medium was removed, and the cells were washed twice with 5 mL of PBS. The cells were then scraped into 0.75 mL of 50 mM potassium phosphate buffer, pH 7.4, containing 250 mM sucrose and 5 μM FAD and sonicated on ice. Protein concentrations of sonicates were determined by the method of Lowry (*35*), and NQO1 activity of sonicates was determined using the reduction of DCPIP at 600 nm (*36*).

NADH Oxidation and Oxygen Consumption. Spectrophotometric analysis of NADH oxidation was performed on a Hewlett-Packard HP8452 diode array spectrophotometer using a quartz cuvette at 32 °C. Reaction conditions (1 mL): buffer, 50 mM potassium phosphate, pH 7.4, containing 3.3 μg/mL rhNQO1, 0.2 mM NADH, and 25 μM indolequinone. Oxygen consumption was measured using a Clark electrode in 3 mL reactions at 32 °C. Reaction conditions (3 mL): buffer, 50 mM potassium phosphate, pH 7.4, containing 125 mM NaCl, 1 mg/mL bovine serum albumin, 3 μg/mL rhNQO1, and 0.5 mM NADH. The oxygen electrode was allowed to equilibrate in buffer for 5−10 min before the introduction of indolequinone (25 μM). Dissolved oxygen concentrations were adjusted for temperature (32 °C) and altitude (1609 m).

Molecular Docking of the Indolequinone Ligands into NQO1. Molecular docking simulations were performed on an SGI Octane 2 workstation using the Insight II software package (Version 2005; Accelrys Inc., San Diego, CA). The crystallographic coordinates for the 1.8 Å structure of human NQO1 cocrystallized with ES936, PDB code 1KBQ (*29*), were obtained from the RCSB Protein Data Bank. The complex was separated into three components: the physiological dimer of the NQO1 protein, the FAD cofactor, and ES936 structures. Hydrogens were added to the NQO1 protein structure, and the ionizable residues were corrected for physiological pH. The anionic form of the reduced cofactor was constructed from the FAD structure, assigned the correct atom type and bond order, and then merged with the protein structure. The indolequinone structures were constructed from the ES936 structure and assigned the correct atom type and bond order; then each in turn was positioned into the binding site of NQO1, using the coordinated system of the protein. The binding site was defined as whole residues within an interface 6 Å radius subset encompassing the ligand-binding domain, including the FAD cofactor. The potentials and charges of the NQO1−ligand complex were corrected using CVFF (*37*). The Affinity program of Insight II was used for the flexible docking of the indolequinone ligands into the NQO1 active site employing a Monte Carlo search algorithm and using default parameters for the grid setup (*38*), followed by a Discover-based minimization, using the conjugate gradient method (1000 iterations), to allow both the ligand and the binding pocket to optimize interactions. Fifty structural outputs were specified, and the nonbonded interaction energy between the NQO1 structure and the appropriate indolequinone was calculated for each structural frame with a specified cutoff of 8 Å. The Affinity docking program generates a set of structures (50 structural outputs were specified) that fall within energetic and geometric parameters; these structures were then ranked from the result set. The structural frames for the NQO1−indolequinone complexes were evaluated on the basis of the following criteria: the total energy as output by Affinity; the nonbonded interaction energy between the NQO1 protein and the indolequinone, calculated with a specified cutoff of 8 Å; the hydrogen bond interactions between protein and indolequinone; and the positioning of the quinone moiety in the binding site.

Growth Inhibition. Growth inhibition in the human pancreatic MIA PaCa-2 cancer cell line was measured using the MTT colorimetric assay (*39*). In these studies, the MIA PaCa-2 cells were seeded at 2×10^3 cells per well in 96-well plates, in triplicate, for each indolequinone and allowed to attach for 16 h. Medium was removed by aspiration, and the MIA PaCa-2 cells were treated with the appropriate indolequinone (6.25−3200 nM) in complete medium for 4 and 72 h time periods. The medium was removed, and MTT (50 μg) in medium (50 μL) was added to each well and incubated for a further 4 h. Cell viability was determined by measuring the cellular reduction of MTT to the crystalline formazan product, dissolved by the addition of DMSO (100 μL). Optical density was determined at 550 nm using a Molecular Devices Thermomax microplate reader. The IC_{50} values were defined as the concentration of indolequinone

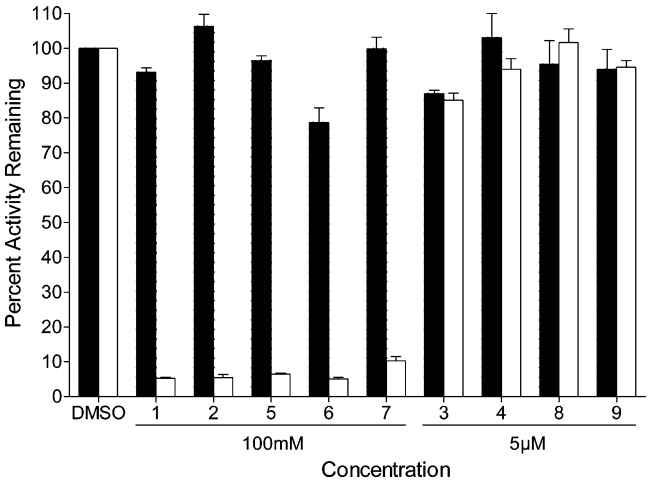

FIGURE 2: Effect of NADH on inhibition of NQO1 by indolequinones. rhNQO1 (1 μg) was incubated with indolequinones **1**, **2**, **5**, **6**, **7** (100 nM) or **3**, **4**, **8**, **9** (5 μM) in the absence (closed bars) and presence (open bars) of 0.2 mM NADH for 5 min, after which an aliquot was removed, diluted 100-fold, and then assayed for NQO1 catalytic activity using the reduction of DCPIP. Results are expressed as the mean (±standard deviation) of three independent determinations.

that resulted in 50% reduction in cell number compared to the DMSO-treated control, determined from semilogarithmic plots of percentage of control versus indolequinone concentration.

RESULTS

The indolequinones in this series were designed to undergo varying degrees of NQO1-mediated reduction to the hydroquinone, with subsequent elimination of a leaving group from the (indol-3-yl)methyl position, generating a reactive iminium ion species. The reactive iminium ion directly alkylates the NQO1 protein within the FAD site, resulting in the irreversible inhibition of NQO1 enzymatic activity. An important measure of mechanism-based inactivation is the requirement for the catalytic step to occur prior to inactivation of the enzyme. The inhibition of rhNQO1 activity by this series of indolequinones was therefore monitored in the presence and absence of NADH to determine if the inhibition of rhNQO1 was mechanism-based (Figure 2). NQO1 inactivation by ES936 has been previously reported (*28*−*31*), but here we also report mechanism-based inhibition of NQO1 with the 6-methoxy analogue **2**. The interactions of **3** and **8** have also been reported previously (*29*−*31*) but were included as comparisons for the 6-methoxy analogues **4** and **9**. The incubation of **1** (ES936), **2**, **5**, **6**, and **7** with NADH and rhNQO1 resulted in approximately 90% inhibition of enzyme activity, and this inactivation was dependent upon NADH, indicative of mechanism-based inhibition as previously reported for ES936 (*29*). No inhibition of rhNQO1 was observed with the indolequinones **3**, **4**, **8**, and **9** in the absence or presence of NADH, and no oxidation of NADH was observed in the absence of NQO1, indicating that **3**, **4**, **8**, and **9** may be substrates for rhNQO1-mediated reduction generating their respective hydroquinones with no subsequent inhibition of rhNQO1. The NQO1-mediated reduction of **3**, **4**, **8**, and **9** was analyzed spectrophotometrically by monitoring the oxidation of NADH (Figure 3A,C; data shown for indolequinones **4** and **9**, equivalent data for **3** and **8** not shown). Furthermore, oxygen consumption studies (Clark electrode) confirmed that the metabolism of the indolequinones **3**, **4**, **8**, and **9** resulted in an immediate nonstoichiometric increase in oxygen consumption, relative to NADH oxidation, demonstrating that these compounds undergo NQO1-mediated redox cycling. The indolequinone alcohols **8** and **9** were efficiently metabolized by NQO1 displaying an increased rate of NADH oxidation and oxygen consumption, in comparison to the inefficient indolequinone substrates, **3** and **4** (Figure 3B,D; data shown for indolequinones **4** and **9**, equivalent data for **3** and **8** not shown). The poor 3-hydroxy and 3-phenoxy leaving groups (*32*) of **3**, **4**, **8**, and **9** are not efficiently eliminated upon NQO1-mediated reduction, and the hydroquinone is autoxidized to the parent quinone at a faster rate than elimination; therefore, the electrophilic iminium ion is not formed, and no alkylation to amino acid residues within the active site of NQO1 occurs. Conversely, the rate of autoxidation of the hydroquinones of **1**, **2**, **5**, **6**, and **7** is too slow to prevent the reductive elimination of the 4-nitrophenoxy, 4-pyridinyloxy, or acetoxy leaving groups (*32*). The partition ratio for a mechanism-based inhibitor is the number of catalytic cycles required to inactivate one molecule of enzyme (*40*); therefore, the lower the partition ratio, the more efficient the inhibitor. To compare the efficiency at which these indolequinones inactivate NQO1, the partition ratio for each indolequinone that demonstrated NADH-dependent NQO1 inhibition was determined. The partition ratios for **1** (ES936) and **2** were 3.5 and 3.7, respectively, while the partition ratios for **5** and **6** were 1.3 and 0.9, respectively, indicating that these indolequinones were efficient NQO1 mechanism-based inhibitors. The 3-acetoxy compound, **7**, had a partition ratio of 45.4, displaying less efficient mechanism-based NQO1 inhibition. The partition ratios for the indolequinones **3**, **4**, **8**, and **9** were not determined since they did not inhibit NQO1. We next examined whether the partition ratios for NQO1 inhibition using purified recombinant human NQO1 reflected NQO1 inhibition in cellular systems. The concentration dependence of NQO1 inhibition after treatment of MIA PaCa-2 cells with compounds **1**, **2**, **6**, and **7** was determined after 1 h (Figure 4). The relative potency of the indolequinones as determined by partition ratios was reflected in their ability to inhibit NQO1 in cells, with compound **6** (partition ratio = 0.9) being most effective and the acetoxy derivative, compound **7** (partition ratio = 45.4), being least effective.

The computational-based molecular docking simulations performed in this study indicate that the human NQO1 protein can accommodate a range of indolequinone substitutions and a variety of binding modes and interactions within the active site. (The structural frames and associated energies from these docking studies are presented in the Supporting Information.) The binding conformations of ES936 and the iminium ion intermediate in both the quinone and hydroquinone forms in the active site of NQO1 containing the oxidized FAD cofactor were examined (Figure 5). In these simulations, the hydroquinone form of ES936 is a more realistic representation since the quinone form of ES936 cannot undergo NQO1-mediated reduction because the cofactor is not in its reduced form. The high-scoring conformations of ES936 in both the quinone and hydroquinone form (Figure 5A,B) were similar to the cocrystallized NQO1−ES936 structure (*29*). The conformations of the

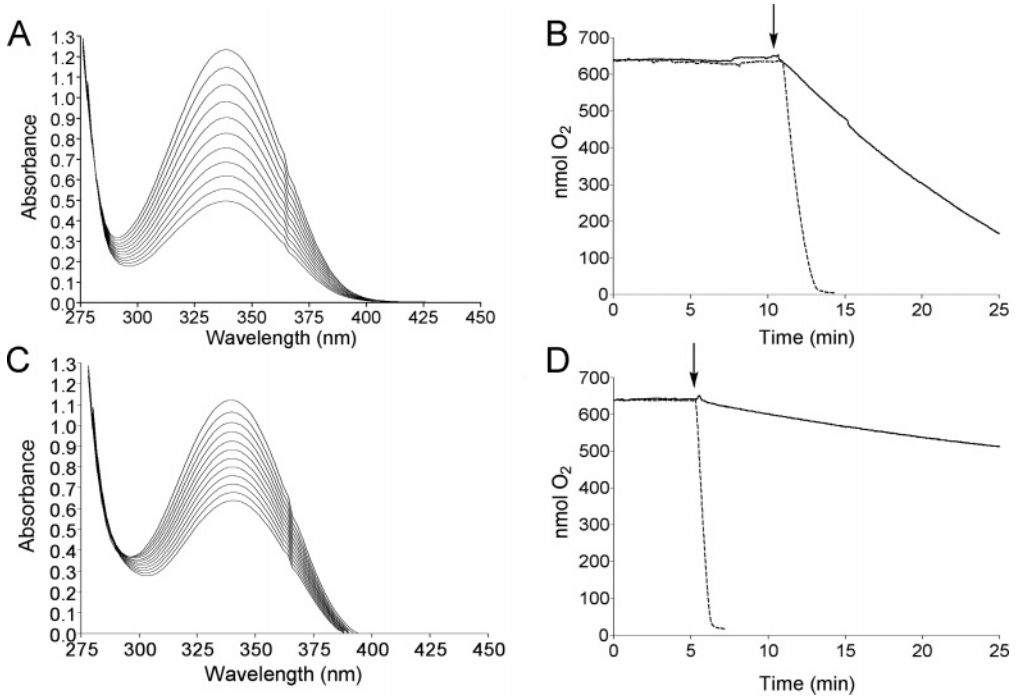

FIGURE 3: NADH oxidation and oxygen consumption during the reduction of indolequinones by NQO1. Spectrophotometric analysis of NADH oxidation (decreased absorbance 340 nm) during the reduction of (A) **9** and (C) **4** by rhNQO1. Scans were recorded (A) every 30 s for 5 min or (C) every 5 min for 1 h at 32 °C. No NADH oxidation was observed in the absence of rhNQO1. Oxygen consumption was measured during the reduction of (B) **9** and (D) **4** by rhNQO1. Polargraphic data were obtained using a Clark electrode. Arrows indicate the addition of 25 μM indolequinone. β-Lapachone (25 μM, dotted line, positive control) was analyzed in separate reactions.

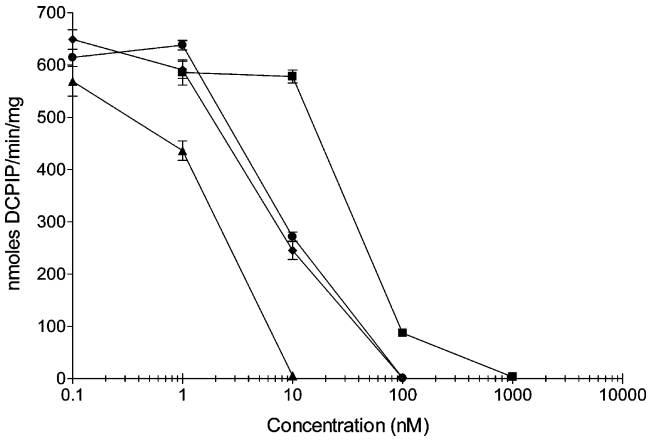

FIGURE 4: Inhibition of NQO1 catalytic activity in Mia PaCa-2 cells treated with indolequinones. Mia PaCa-2 cells were treated with indolequinones (**1**, **2**, **6**, and **7**) at the indicated concentrations in complete growth medium for 1 h, after which cells were harvested and NQO1 catalytic activity was measured using the reduction of DCPIP. Results are the mean (±standard deviation) of three independent determinations. Closed circles, **1**; closed diamonds, **2**; closed triangles, **6**; closed squares, **7**.

quinone and hydroquinone iminium ion intermediates (Figure 5C,D) were comparable to each other and display interactions with Tyr128 and suggest, from this theoretical simulation, that alkylation could be directed to the Tyr128 residue, due to the proximity of the reactive methide; this is in agreement with previous mass spectroscopic approaches (*29*). Molecular docking simulations were also performed for the indolequinone series using NQO1 with the anionic form of the reduced isoalloxazine ring cofactor (*41*, *42*) with the negative charge on N1 and O2 in the keto form. From these docking simulations two reoccurring, high-scoring binding conformations were observed for this series of indolequinones (Figure 6). The first mirrored that of the resolved crystal structure for ES936 in complex with NQO1 (*29*) with hydrogen bonding observed between the C7 carbonyl of the quinone and Tyr126 (Figure 6A,C). In the second, lower energy and highest ranked binding conformation, the C4 carbonyl of the quinone hydrogen bonds to the hydroxyl of Tyr128, and the C7 carbonyl hydrogen bonds to the N5-H of the reduced isoalloxazine ring (Figure 6B,D). Low interaction energies were obtained for this indolequinone series, when the indolequinone moiety lies parallel over the anionic form of the reduced isoalloxazine ring system of the flavin cofactor, displaying interactions between the 4,7-carbonyl groups of the indolequinone and Tyr126 or Tyr128, and the 4-nitrophenoxy, phenoxy, or 4-pyridinyloxy substituent interacts with the hydrophobic Phe232, Phe236, and Tyr128 residues. The acetoxy and 3-hydroxymethyl indolequinones **7**, **8**, and **9** can adopt a number of conformations in the NQO1 active site; however, those which were positioned in parallel to the isoalloxazine ring resulted in low interaction energies although higher than those of **1**−**6**. This higher interaction energy for **7**, **8**, and **9** is due to the lack of a bulky aromatic substituent at the 3-position to anchor the indolequinone in the active site and to interact with hydrophobic residues, such as Phe232, Phe236, and Tyr128, reducing the van der Waals contribution to the interaction energy with an uncompensatory decrease in electrostatic energy. Overall, these indolequinone docking studies support the model in which quinones with attached aromatic rings are positioned in the active site so as to optimize aromatic $\pi-\pi$ interactions (*43*, *44*) with the reduced isoalloxazine ring system of the cofactor (*41*, *42*), which was reflected in the van der Waals contribution to the interaction energy.

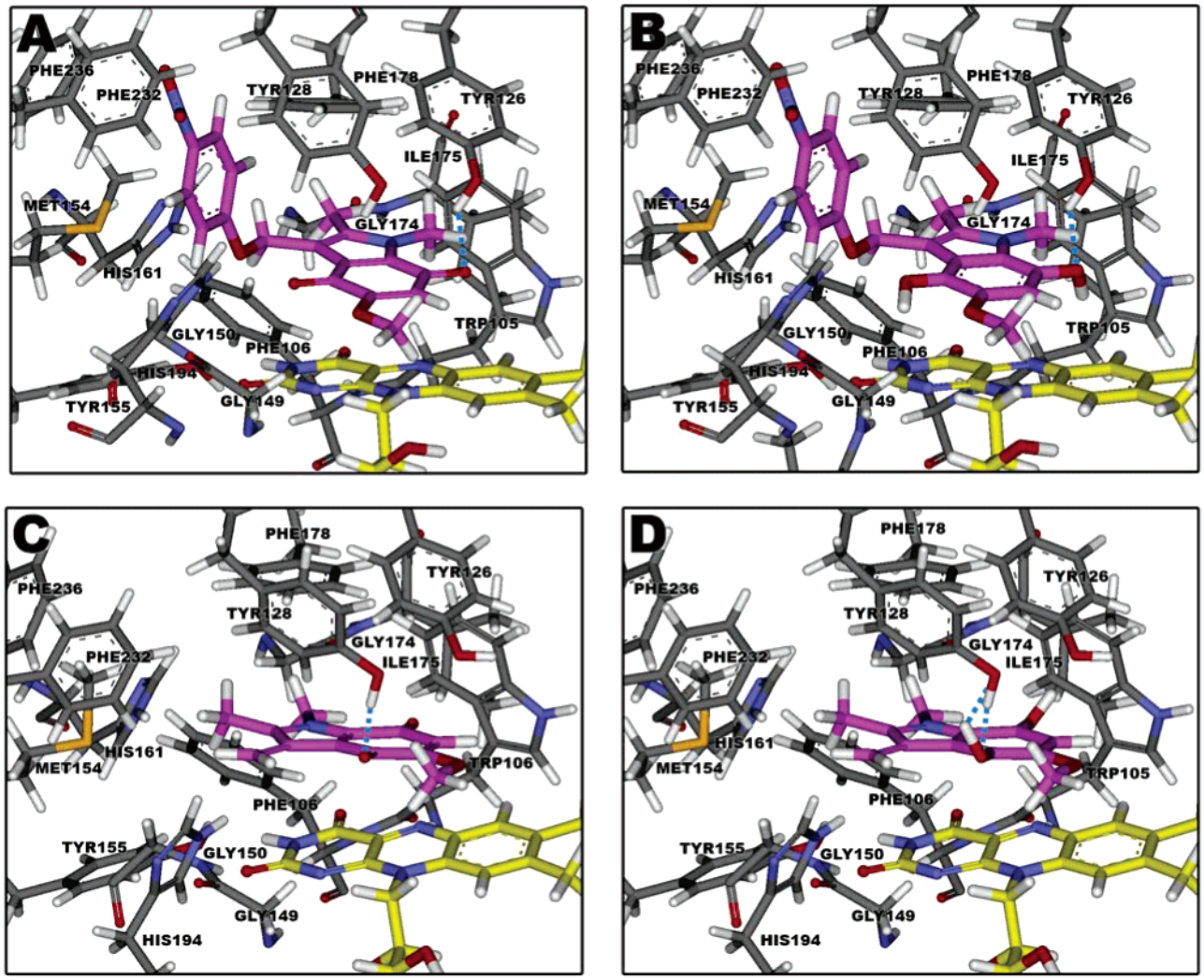

FIGURE 5: Structural frames from molecular docking simulations of ES936 in the active site of NQO1. Representations of ES936 (**1**) in the (A) quinone, (B) hydroquinone, (C) quinone methide, and (D) hydroquinone methide forms (stick display style; colored by atom type, carbon atoms colored salmon) in the oxidized FAD (stick display style; colored by atom type, carbon atoms colored yellow) site of NQO1, key amino acids (stick display style; colored by atom type), and hydrogen bond contacts (blue dashed lines) are displayed. The figures were constructed using Discovery Studio Visualizer (Accelrys, Inc., San Diego, CA).

Inhibition of NQO1 in cellular systems was examined to verify inhibition of NQO1, the proposed intracellular target of these compounds, and ensure that compounds were taken up into cells. Importantly, the indolequinones **1** (ES936), **2**, **5**, **6**, and **7** (100 nM) efficiently inhibited NQO1 activity (>90%) in the human pancreatic MIA PaCa-2 solid tumor cell line, after 4 h (Figure 7). Because of the essentially total inhibition of NQO1 by these compounds after 4 h, this time point was selected for growth inhibition studies in the MIA PaCa-2 cell line. A longer exposure period (72 h) was also used for comparative purposes, and the IC_{50} values are reported for both 4 and 72 h treatments with the appropriate indolequinone (Table 1). After 4 h of incubation in MIA PaCa-2 cells compounds **1**, **2**, **5**, **6**, and **7** (100 nM) demonstrated essentially complete inhibition of NQO1 (>90%). Examination of the growth inhibitory potency of the compounds after 4 h of incubation indicates that compounds **1** and **2** were effective inhibitors of growth in MIA Paca-2 cells while compounds **5**, **6**, and **7** were not. These data indicate dissociation of NQO1 inhibitory activity and the ability to induce growth inhibition in MIA PaCa-2 cells. Interestingly, the noninhibitory analogues, compounds **3** and **4**, demonstrated decreases in IC_{50} value after 72 h relative to 4 h of incubation with cells, and the change with compound **4** was dramatic from 4563 to 409.4 nM. This finding indicates that compounds **3** and **4** function via an NQO1-independent mechanism to potently inhibit cell proliferation after 72 h of treatment. The indolequinones **8** and **9**, the potential terminal metabolites of indolequinones **1**−**7**, generated by reaction of the putative iminium ion intermediate with water, were poor inhibitors of cell growth. In addition, the effect of 4-nitrophenol and 4-hydroxypyridine on growth inhibition was also examined, and both were found to be relatively nontoxic.

DISCUSSION

In this report, we have examined a series of indolequinones as mechanism-based inhibitors of NQO1 and studied their NQO1 inhibitory properties in cell-free, cell-based, and in silico systems. The effect of NQO1 inhibition in pancreatic cancer as a potential therapeutic strategy has been hindered, to date, by the lack of specific and potent NQO1 inhibitors. In this study, we have demonstrated that NQO1-mediated reductive elimination of an efficient leaving group from the

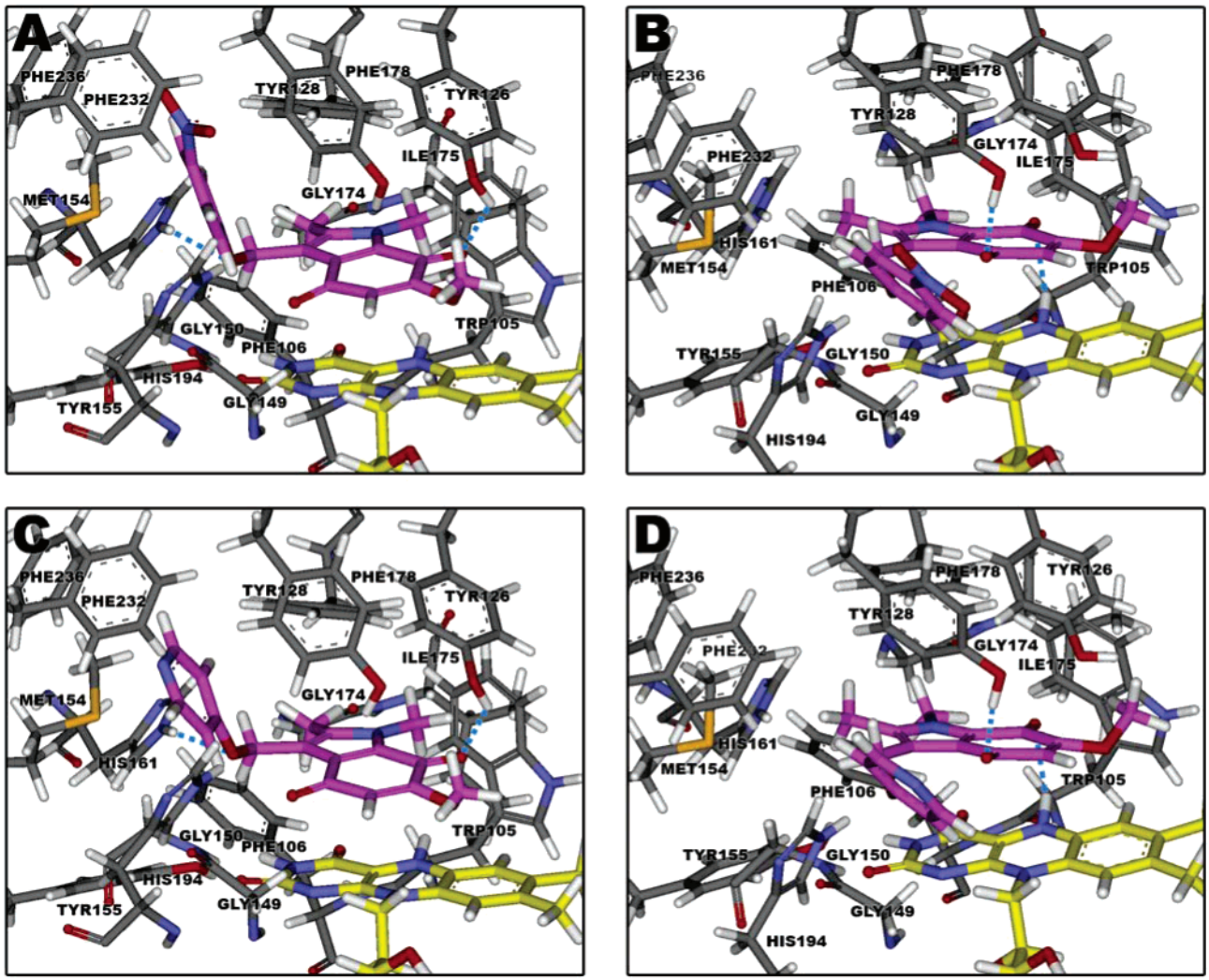

FIGURE 6: Structural frames from molecular docking simulations of the indolequinone ligands **2** and **6** in the active site of NQO1. Representations of the indolequinones (A) **2**, frame 1, (B) **2**, frame 4, (C) **6**, frame 1, and (D) **6**, frame 2 (stick display style; colored by atom type, carbon atoms colored salmon), in the reduced FAD (stick display style; carbon atoms colored yellow) site of NQO1, key amino acids (stick display style; colored by atom type), and hydrogen bond contacts (blue dashed lines) are displayed. The figures were constructed using Discovery Studio Visualizer (Accelrys, Inc., San Diego, CA).

3-position of the indolequinone can result in NQO1 mechanism-based inhibition. The indolequinones, in this series, with 4-nitrophenoxy, 4-pyridinyloxy, and acetoxy substituents at the (indol-3-yl)methyl position were inhibitors of NQO1, and inhibition was NADH-dependent, indicative of mechanism-based inhibition. However, the indolequinones with hydroxy and phenoxy substituents at the 3-position were not inhibitors of NQO1, presumably due to the poorer leaving group ability of hydroxide and phenoxide, respectively. The nature of the leaving group appears to be a critical determinant for NQO1 inhibition and potentially the toxicity of these indolequinone-based compounds. One measure of leaving group ability is the strength of its conjugate acid as measured by its pK_a value; the lower the pK_a, the better the leaving group. The pK_a of 4-nitrophenol is 7.1 (in water) and 10.8 (in DMSO), 4-hydroxypyridine is 5.18 (in water) and 14.8 (in DMSO), and acetic acid is 4.76 (in water) and 12.3 (in DMSO) (*45*−*48*), indicative of good leaving groups, which correlates to efficient inhibition of rhNQO1 and NQO1 in MIA PaCa-2 cells. The pK_a of water is 15.7 (water) and 31.2 (DMSO) and phenol is 9.96 (water) and 18.0 (DMSO) (*45*, *49*, *50*), indicating that the hydroxy and phenoxy substituents at the (indol-3-yl)methyl position would be poorer leaving groups, which corresponds to the poor NQO1 inhibitory properties of **3**, **4**, **8**, and **9**. Importantly, the relative potency of the NQO1 inhibitory indolequinones, as measured by partition ratio, reflected their ability to inhibit NQO1 in MIA PaCa-2 cells.

The available crystal structures of NQO1, and previous molecular docking studies examining the binding modes of various quinones, maintain the FAD cofactor in the oxidized form. The oxidized form of FAD represents the state of the cofactor at the beginning of the catalytic cycle. To accept a quinone substrate, a hydride ion from NAD(P)H is first transferred to the N5 flavin nitrogen with a proposed charge stabilization from a catalytic triad involving the FAD cofactor, His161, and Tyr155 (*41*, *42*). The hydride is then available for donation from the N5 of the isoalloxazine ring to the quinone substrate with the remaining hydrogen coming from Tyr126 or Tyr128 directly or through interaction with water. A previous study, examining the structural optimization of the isolated and NQO1-bound isoalloxazine ring in both the oxidized and reduced forms of FAD (*41*), demonstrated that the protein environment imposes a planar

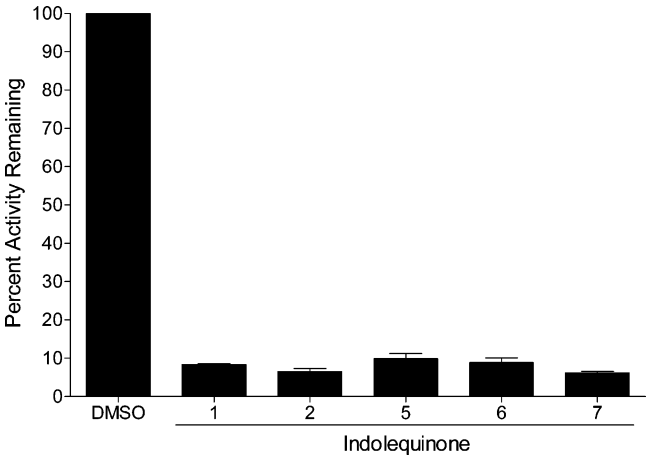

FIGURE 7: Inhibition of NQO1 activity in Mia PaCa-2 cells by indolequinones. NQO1 activity was measured in Mia PaCa-2 sonicates following a 4 h exposure to DMSO (control) or indolequinone (100 nM) in complete media. Results are expressed as the mean ± standard deviation, $n = 3$.

Table 1: IC_{50} Values for Growth Inhibition Induced by Indolequinones in MIA PaCa-2 Cells[a]

compound	IC_{50} (nM) 4 h	IC_{50} (nM) 72 h
1 (ES936)	629.2 ± 16.7	507.8 ± 5.2
2	638.4 ± 14.8	354.5 ± 3.2
3	1385 ± 24.4	962.2 ± 18.4
4	4563 ± 25.6	409.4 ± 30.2
5	2007 ± 16.4	2172 ± 25.3
6	2562 ± 7.4	3121 ± 14.7
7	2422 ± 9.8	2160 ± 12.0
8	2154 ± 27.3	1985 ± 10.2
9	2174 ± 11.1	2162 ± 19.1
4-nitrophenol	NC[b]	NC[b]
4-hydroxypyridine	NC[b]	NC[b]

[a] Calculated IC_{50} values are the mean of three independent determinations. [b] NC denotes no convergence.

structure on the reduced isoalloxazine ring. This stabilizes the geometry and electrostatic potential through multiple interactions with charged amino acid residues of the protein thus maintaining a negative reduction potential and offering an explanation as to how NQO1 can efficiently metabolize a range of quinone substrates. Therefore, in molecular docking simulations the reduced form of the FAD cofactor should be used when examining the binding conformation of a quinone substrate in the NQO1 active site, since it results in a more accurate representation of the ligand-binding conformation due to differences in electronic interactions between the reduced cofactor and quinone substrate.

The theoretical molecular docking simulations of this indolequinone series, in the anionic reduced FAD site of NQO1, resulted in conformations similar to those in the resolved cocrystallized structures of NQO1 in complex with ES936 or **3** (*29*). This conformation was one of two high-scoring conformations and could be the initial binding conformation of the indolequinone in the active site. The rotation of the indolequinone would result in the alternate lower energy binding conformation with the quinone carbonyl aligned with N5-H of the reduced flavin and Tyr128, for hydride transfer. This mechanism could explain why large substituents at the N1 and/or C2 positions of indolequinone result in different binding conformations, in that the amino acid residues, Gly174, Ile175, Trp105, and Phe106 in the active site, will not allow for this rotation and therefore adopt a different orientation in the NQO1 active site (*31*). The examination of these binding modes and interactions may direct the further development of indolequinone-based NQO1 inhibitors. In both conformations the plane of the indolequinone lies parallel to the isoallozaxine ring, which forms the base of the catalytic domain, optimizing aromatic $\pi-\pi$ interactions and consequently increasing the van der Waals contribution to the interaction energy resulting in low interaction energies. Interestingly, in the docking simulations and subsequent minimizations using the reduced anionic FAD cofactor, the isoalloxazine ring structure remains planar; however, the hydrogen at N5 is raised toward the indolequinone ligand. The aromatic substituents of **1**−**6** at the (indol-3-yl)methyl position are positioned almost perpendicular to the indolequinone interacting with hydrophobic residues, such as Phe232, Phe236, and Tyr128, further increasing the van der Waals contribution to the interaction energy. The two binding conformations for the phenoxy compounds **3** and **4** result in low interaction energies, comparable to those of **1**, **2**, **5**, and **6** due to similar global interactions; therefore, when examining the binding conformations of indolequinones, the nature of the leaving group needs to be considered.

The indolequinones in this series, both NQO1 inhibitory and noninhibitory, allowed us to test the hypothesis that NQO1 inhibition was required for growth inhibitory activity in pancreatic cancer cells. Using the 4 h time point where we verified essentially total inhibition of NQO1 activity, we examined the ability of the NQO1 inhibitory indolequinone analogues to induce growth inhibition. The pyridinyloxy and acetoxy compounds **5**, **6**, and **7**, which were potent inhibitors of NQO1 activity after 4 h of incubation, were relatively poor inhibitors of cell proliferation, suggesting a lack of correlation of NQO1 inhibitory activity and growth inhibition. This analysis is predicated on the use of a single concentration of compound (100 nM) to examine NQO1 inhibitory activity in MIA PaCa-2 cells, after 4 h. The IC_{50} values for growth inhibitory activity of compounds **5**, **6**, and **7** measured at 4 h were at least 20-fold higher (2000 nM), ensuring effective inhibition of NQO1 under these conditions. An alternative method to examine the relationship between NQO1 inhibitory activity and growth inhibitory activity is to utilize the measured partition ratios of the indolequinones for NQO1 inhibition. This method also demonstrates dissociation of NQO1 inhibition and growth inhibition since the most potent NQO1 inhibitory compounds as reflected by partition ratio are compounds **5** and **6**, which are not effective at inducing growth inhibition. The use of a second time point of 72 h for MTT analysis also proved useful to test the overall hypothesis that NQO1 inhibition was required for growth inhibitory activity. The phenoxy compounds **3** and **4** were not inhibitors of NQO1 enzymatic activity nor good substrates for NQO1 but demonstrated potent growth inhibition at 72 h, suggestive of an NQO1-independent mechanism of action. Collectively, our data demonstrate that NQO1 inhibition can be dissociated from the growth inhibitory activity of this series of indolequinones in the human pancreatic MIA PaCa-2 tumor cell line.

In summary, we have examined a series of indolequinones and evaluated their capacity to inhibit NQO1 in cell-free,

cell-based, and in silico systems and their ability to inhibit cell proliferation in the human pancreatic MIA PaCa-2 cancer cell line. We have characterized new mechanism-based inhibitors of NQO1 and shown that their partition ratios reflect their ability to inhibit NQO1 in cells. Our data demonstrate that NQO1 inhibition does not correlate with growth inhibitory activity in MIA PaCa-2 cells, suggesting that targets in addition to NQO1 need to be considered to explain the potent activity of this series of indolequinones in human pancreatic cancer cells.

SUPPORTING INFORMATION AVAILABLE

Data from the molecular docking simulations and structural frames and associated energies from the docking studies listed with the highest ranked complex highlighted for each simulation. This material is available free of charge via the Internet at http://pubs.acs.org.

REFERENCES

1. Ross, D. (2004) Quinone reductases multitasking in the metabolic world, *Drug Metab. Rev. 36*, 639−654.
2. Powis, G., Svingen, B. A., and Appel, P. (1981) Quinone-stimulated superoxide formation by subcellular fractions, isolated hepatocytes, and other cells, *Mol. Pharmacol. 20*, 387−394.
3. Chesis, P. L., Levin, D. E., Smith, M. T., Ernster, L., and Ames, B. N. (1994) Mutagenicity of quinones: pathways of metabolic activation and detoxification, *Proc. Natl. Acad. Sci. U.S.A. 81*, 1696−1700.
4. Lind, C., Hochstein, P., and Ernster, L. (1982) DT-diaphorase as a quinone reductase: a cellular control device against semiquinone and superoxide radical formation, *Arch. Biochem. Biophys. 216*, 178−185.
5. Workman, P. (1994) Enzyme-directed bioreductive drug development revisited: a commentary on recent progress and future prospects with emphasis on quinone anticancer agents and quinone metabolizing enzymes, particularly DT-diaphorase, *Oncol. Res. 6*, 461−475.
6. Ross, D., Siegel, D., Beall, H., Prakash, A. S., Mulcahy, R. T., and Gibson, N. W. (1993) DT-diaphorase in activation and detoxification of quinones. Bioreductive activation of mitomycin C, *Cancer Metastasis Rev. 12*, 83−101.
7. Siegel, D., and Ross, D. (2000) Immunodetection of NAD(P)H: quinone oxidoreductase 1 (NQO1) in human tissues, *Free Radical Biol. Med. 29*, 246−253.
8. Malkinson, A. M., Siegel, D., Forrest, G. L., Gazdar, A. F., Oie, H. K., Chan, D. C., Bunn, P. A., Mabry, M., Dykes, D. J., and Harrison, S. D. (1992) Elevated DT-diaphorase activity and messenger RNA content in human non-small cell lung carcinoma: relationship to the response of lung tumor xenografts to mitomycin C, *Cancer Res. 52*, 4752−4757.
9. Schlager, J. J., and Powis, G. (1990) Cytosolic NAD(P)H:(quinone-acceptor) oxidoreductase in human normal and tumor tissue: effects of cigarette smoking and alcohol, *Int. J. Cancer 45*, 403−409.
10. Lyn-Cook, B. D., Yan-Sanders, Y., Moore, S., Taylor, S., Word, B., and Hammons, G. J. (2006) Increased levels of NAD(P)H: quinone oxidoreductase 1 (NQO1) in pancreatic tissues from smokers and pancreatic adenocarcinomas: A potential biomarker of early damage in the pancreas, *Cell Biol. Toxicol. 22*, 73−80.
11. Logsdon, C. D., Simeone, D. M., Binkley, C., Arumugam, T., Greenson, J. K., Giordano, T. J., Misek, D. E., Kuick, R., and Hanash, S. (2003) Molecular profiling of pancreatic adenocarcinoma and chronic pancreatitis identifies multiple genes differentially regulated in pancreatic cancer, *Cancer Res. 63*, 2649−2657.
12. Jemal, A., Thomas, A., Murray, T., and Thun, M. (2002) Cancer statistics, 2002, *CA Cancer J. Clin. 52*, 23−47.
13. Boring, C. C., Squires, T. S., and Tong, T. (1993) Cancer statistics, 1993, *CA Cancer J. Clin. 43*, 7−26.
14. Edwards, B. K., Howe, H. L., Ries, L. A., Thun, M. J., Rosenberg, H. M., Yancik, R., Wingo, P. A., Jemal, A., and Feigal, E. G. (2002) Annual report to the nation on the status of cancer, 1973−1999, featuring implications of age and aging on U.S. cancer burden, *Cancer 94*, 2766−2792.
15. Gold, E. B., Gordis, L., Diener, M. D., Seltser, R., Boitnott, J. K., Bynum, T. E., and Hutcheon, D. F. (1985) Diet and other risk factors for cancer of the pancreas, *Cancer 55*, 460−467.
16. Durbec, J. P., Chevillotte, G., Bidart, J. M., Berthezene, P., and Sarles, H. (1983) Diet, alcohol, tobacco and risk of cancer of the pancreas: a case-control study, *Br. J. Cancer 47*, 463−470.
17. Bouvet, M., Binmoeller, K. F., and Moossa, A. R. (2000) Diagnosis of adenocarcinoma of the pancreas, in *American Cancer Society atlas of clinical oncology*: *pancreatic cancer* (Cameron, J. L., Ed.) BC Decker, Hamilton, Ontario, Canada.
18. Jemal, A., Murray, T., Samuels, A., Ghafoor, A., Ward, E., and Thun, M. J. (2003) Cancer statistics, 2003, *CA Cancer J. Clin. 53*, 5−26.
19. Yeo, C. J., and Cameron, J. L. (1999) Pancreatic cancer, *Curr. Probl. Surg. 36*, 59−152.
20. Bramhall, S. R., Allum, W. H., Jones, A. G., Allwood, A., Cummins, C., and Neoptolemos, J. P. (1995) Treatment and survival in 13,560 patients with pancreatic cancer, and incidence of the disease, in the West Midlands: an epidemiological study, *Br. J. Surg. 82*, 111−115.
21. Neoptolemos, J. P., Stocken, D. D., Friess, H., Bassi, C., Dunn, J. A., Hickey, H., Beger, H., Fernandez-Cruz, L., Dervenis, C., Lacaine, F., Falconi, M., Pederzoli, P., Pap, A., Spooner, D., Kerr, D. J., and Buchler, M. W. (2004) European Study Group for Pancreatic Cancer. A randomized trial of chemoradiotherapy and chemotherapy after resection of pancreatic cancer, *N. Engl. J. Med. 350*, 1200−1210.
22. Cullen, J. J., Hinkhouse, M. M., Grady, M., Gaut, A. W., Liu, J., Zhang, Y. P., Weydert, C. J., Domann, F. E., and Oberley, L. W. (2003) Dicumarol inhibition of NADPH:quinone oxidoreductase induces growth inhibition of pancreatic cancer via a superoxide-mediated mechanism, *Cancer Res. 63*, 5513−5520.
23. Siegel, D., Gustafson, D. L., Dehn, D. L., Han, J. Y., Boonchoong, P., Berliner, L. J., and Ross, D. (2004) NAD(P)H:quinone oxidoreductase 1: role as a superoxide scavenger, *Mol. Pharmacol. 65*, 1238−1247.
24. Mays, J. B., and Benson, A. M. (1992) Inhibition of mouse glutathione transferases and glutathione peroxidase II by dicumarol and other ligands, *Biochem. Pharmacol. 44*, 921−925.
25. Segura-Aguilar, J. E., Barreiro, V., and Lind, C. (1986) Dicoumarol-sensitive glucuronidation of benzo(a)pyrene metabolites in rat liver microsomes, *Arch. Biochem. Biophys. 251*, 266−275.
26. Cross, J. V., Deak, J. C., Rich, E. A., Qian, Y., Lewis, M., Parrott, L. A., Mochida, K., Gustafson, D., Vande Pol, S., and Templeton, D. J. (1999) Quinone reductase inhibitors block SAPK/JNK and NFkappaB pathways and potentiate apoptosis, *J. Biol. Chem. 274*, 31150−31154.
27. Wadkins, C. L., and Lehninger, A. L. (1958) The adenosine triphosphate-adenosine diphosphate exchange reaction of oxidative phosphorylation, *J. Biol. Chem. 233*, 1589−1597.
28. Dehn, D. L., Siegel, D., Swann, E., Moody, C. J., and Ross, D. (2003) Biochemical, cytotoxic, and genotoxic effects of ES936, a mechanism-based inhibitor of NAD(P)H:quinone oxidoreductase 1, in cellular systems, *Mol. Pharmacol. 64*, 714−720.
29. Winski, S. L., Faig, M., Bianchet, M. A., Siegel, D., Swann, E., Fung, K., Duncan, M. W., Moody, C. J., Amzel, L. M., and Ross, D. (2001) Characterization of a mechanism-based inhibitor of NAD(P)H:quinone oxidoreductase 1 by biochemical, X-ray crystallographic, and mass spectrometric approaches, *Biochemistry 40*, 15135−15142.
30. Swann, E., Barraja, P., Oberlander, A. M., Gardipee, W. T., Hudnott, A. R., Beall, H. D., and Moody, C. J. (2001) Indolequinone antitumor agents: correlation between quinone structure and rate of metabolism by recombinant human NAD(P)H:quinone oxidoreductase. Part 2, *J. Med. Chem. 44*, 3311−3319.
31. Beall, H. D., Winski, S., Swann, E., Hudnott, A. R., Cotterill, A. S., O'Sullivan, N., Green, S. J., Bien, R., Siegel, D., Ross, D., and Moody, C. J. (1998) Indolequinone antitumor agents: correlation between quinone structure, rate of metabolism by recombinant human NAD(P)H:quinone oxidoreductase, and *in vitro* cytotoxicity, *J. Med. Chem. 41*, 4755−4766.
32. Everett, S. A., Naylor, M. A., Barraja, P., Swann, E., Patel, K. B., Stratford, M. R. L., Hudnott, A. R., Vojnovic, B., Locke, R. J., Wardman, P., and Moody, C. J. (2001) Controlling the rates of reductive elimination from the (indol-3-yl)methyl position of indolequinones, *J. Chem. Soc., Perkin Trans. 2*, 843−860.
33. Dehn, D. L., Siegel, D., Zafar, K. S., Reigan, P., Swann, E., Moody, C. J., and Ross, D. (2006) 5-Methoxy-1,2-dimethyl-3-[(4-nitrophenoxy)methyl]indole-4,7-dione, a mechanism-based

inhibitor of NAD(P)H:quinone oxidoreductase 1, exhibits activity against human pancreatic cancer *in vitro* and *in vivo*, *Mol. Cancer Ther. 5*, 1702−1709.
34. Beall, H. D., Mulcahy, R. T., Siegel, D., Traver, R. D., Gibson, N. W., and Ross, D. (1994) Metabolism of bioreductive antitumor compounds by purified rat and human DT-diaphorases, *Cancer Res. 54*, 3196−3201.
35. Lowry, O. H., Rosebrough, N. J., Farr, A. L., and Randall, R. J. (1951) Protein measurement with the Folin phenol reagent, *J. Biol. Chem. 193*, 265−275.
36. Benson, A. M., Hunkeler, M. J., and Talalay, P. (1980) Increase of NAD(P)H:quinone reductase by dietary antioxidants: possible role in protection against carcinogenesis and toxicity, *Proc. Natl. Acad. Sci. U.S.A. 77*, 5216−5220.
37. Dauber-Osguthorpe, P., Roberts, V. A., Osguthorpe, D. J., Wolff, J., Genest, M., and Hagler, A. T. (1988) Structure and energetics of ligand binding to proteins: *Escherichia coli* dihydrofolate reductase-trimethoprim, a drug-receptor system, *Proteins 4*, 31−47.
38. Luty, B. A., Wasserman, Z. R., Stouten, P. F. W., Hodge, C. N., Zacharias, M., and McCammon, J. A. (1995) A molecular mechanics/grid method for evaluation of ligand-receptor interactions, *J. Comput. Chem. 16*, 454−464.
39. Mosmann, T. (1983) Rapid colorimetric assay for cellular growth and survival: application to proliferation and cytotoxicity assays, *J. Immunol. Methods 65*, 55−63.
40. Silverman, R. B. (1988) Mechanism based enzyme inactivation, in *Chemistry and Enzymology*, Vol. 1, CRC Press, Boca Raton, FL.
41. Cavelier, G., and Amzel, L. M. (2001) Mechanism of NAD(P)H: quinone reductase: *Ab initio* studies of reduced flavin, *Proteins 43*, 420−432.
42. Li, R., Bianchet, M. A., Talalay, P., and Amzel, L. M. (1995) The three-dimensional structure of NAD(P)H:quinone reductase, a flavoprotein involved in cancer chemoprotection and chemotherapy: mechanism of the two-electron reduction, *Proc. Natl. Acad. Sci. U.S.A. 92*, 8846−8850.
43. Zhou, Z., Fisher, D., Spidel, J., Greenfield, J., Patson, B., Fazal, A., Wigal, C., Moe, O. A., and Madura, J. D. (2003) Kinetic and docking studies of the interaction of quinones with the quinone reductase active site, *Biochemistry 42*, 1985−1994.
44. Suleman, A., and Skibo, E. B. (2002) A comprehensive study of the active site residues of DT-diaphorase: rational design of benzimidazolediones as DT-diaphorase substrates, *J. Med. Chem. 45*, 1211−1220.
45. Bordwell, F. G. (1988) Equilibrium acidities in dimethyl sulfoxide solution, *Acc. Chem. Res. 21*, 456−463.
46. Marko-Varga1, G., and Barceló, D. (1992) Liquid chromatographic retention and separation of phenols and related aromatic compounds on reversed phase columns, *Chromatographia 34*, 146−154.
47. Barlin, G. B., and Pfleiderer, W. (1971) Ionization constants of heterocyclic substances. Part IX. Protonation of aminopyridones and aminopyrimidones, *J. Chem. Soc. B* 1425−1432.
48. Ivanović, D., Medenica, M., Nivaud-Guernet, E., and Guernet, M. (1995) Effect of pH on the retention behaviour of some preservatives-antioxidants in reversed-phase high-performance liquid chromatography, *Chromatographia 40*, 652−656.
49. Shinkai, S., Hamada, H., Kusano, Y., and Manabe, O. (1979) Coenzyme models. Part 16. Studies of general-acid catalysis in the NADH model reduction, *J. Chem. Soc., Perkin Trans. 2*, 699−702.
50. Warwicker, J. (2004) Improved pK_a calculations through flexibility based sampling of a water-dominated interaction scheme, *Protein Sci. 13*, 2793−2805.

BI700008Y